AIAA 2016-2954
Aeroacoustics Conferences
30 May - 1 June, 2016, Lyon, France
22nd AIAA/CEAS Aeroacoustics Conference

Experimental Investigation of Leading Edge Hook Structures for Wind Turbine Noise Reduction

Thomas F. Geyer*,
Brandenburg University of Technology Cottbus - Senftenberg, 03046 Cottbus, Germany

Sahan H. Wasala†, John E. Cater‡,
University of Auckland, Auckland 1142, New Zealand

Stuart E. Norris§,
University of Auckland, Auckland 1142, New Zealand,

Ennes Sarradj¶
Brandenburg University of Technology Cottbus - Senftenberg, 03046 Cottbus, Germany

The interaction of a turbulent flow with the leading edge of a blade is a main noise source mechanism especially for wind turbines, which are often exposed to intense atmospheric turbulence with a wide range of length scales. The present paper describes an experimental study performed to explore the noise reducing effect of hook-like extensions, which are fixed to the leading edge of a low speed airfoil. The measurements took place in an aeroacoustic wind tunnel using microphone array technique, while simultaneously the aerodynamic performance of the modified airfoils was captured. It was found that the hook structures lead to a noise reduction at low frequencies, while the noise at high frequencies slightly increases. The aerodynamic performance does not change significantly.

List of Symbols

b	[m]	span width
c_l	[m]	chord length
f_c	[s^{-1}]	center frequency
$G_{uu}(f)$	[m^2/s]	one-sided power spectrum of the velocity fluctuations
Ma	[-]	Mach number
L_p	[dB]	sound pressure level
Λ_x	[m]	(streamwise) turbulence length scale
$\hat{\Lambda}_x$	[-]	ratio of (streamwise) turbulence length scale to maximum airfoil thickness
Re	[-]	Reynolds number based on chord length
Sr	[-]	Strouhal number based on chord length
Tu	[%]	turbulence intensity
u	[m/s]	turbulent velocity fluctuations
U	[m/s]	mean (time-averaged) flow velocity
U_0	[m/s]	free stream velocity (flow speed)
x, y, z	[m]	cartesian coordinates

*Research Assistant, Chair of Technical Acoustics, Brandenburg University of Technology Cottbus - Senftenberg, Germany.
†PhD Student, Department of Engineering Science, University of Auckland, New Zealand.
‡Senior Lecturer, Department of Engineering Science, University of Auckland, New Zealand.
§Senior Lecturer, Department of Mechanical Engineering, University of Auckland, New Zealand.
¶Professor, Chair of Technical Acoustics, Brandenburg University of Technology Cottbus - Senftenberg, Germany.

Table 1. **Overview of turbulence grids used in the experiments**

Grid no.	description	mesh width [mm]	bar width [mm]	porosity [%]
1	PPS 12/2	12	2	0.69
2	PPS 14/4	14	4	0.51

I. Introduction

Noise is one of the main reasons for the growing public objection to wind energy industry [1]. Therefore, it is necessary to find efficient methods to reduce noise levels. Wind turbines are often exposed to intense atmospheric turbulence with a wide range of length scales. When these turbulent eddies interact with the blade, noise is generated at the leading edge. This is considered to be a significant noise generation mechanism, especially when the leading edge of the blade is sharp compared to the length scale of the turbulent eddies. Experimental approaches to reduce this turbulence interaction noise mainly focus on modifying the blade geometry, for example through the use of serrated or wavy leading edges [2–7]. Another possible method is the modification of the material of the leading edge, for example by using flow-permeable materials [3, 8]. Besides the experimental work, there are also some numerical approaches. These include serrated and wavy leading edges [9, 10] as well as porous materials [11]. A more recent numerical study was performed on the potential noise reduction of a blade with a leading edge modified with hooks [12]. These hooks were inspired by the extensions that can be found on the first primary feather of owls wing [13].

Past studies of the silent flight of owls suggest that the leading edge hooks rather serve an aerodynamic purpose by controlling separation [14, 15]. A recent investigation [16] supports these findings by showing that at moderate angles of attack the influence of the hooks on the noise reduction is negligible, while at large angles a small noise reduction was observed. Nevertheless, the reduction of turbulence interaction noise through using structures similar to a comb still seems worth examining. The present paper describes an experimental study of the noise generated by airfoils whose leading edges are modified using hook-like extensions. The remainder of this paper is organized as follows: First, the experimental setup will be explained, including the aeroacoustic wind tunnel and the grids used for the generation of turbulence, the airfoils modified with leading edge hook structures, the microphone array measurement technique and the wind tunnel balance used for the measurement of the aerodynamic forces acting on the airfoils. Then, the results of the acoustic and aerodynamic measurements will be presented and discussed. Finally, the findings will be summarized.

II. Experimental Setup

II.A. Wind Tunnel

The measurements took place in the small aeroacoustic open jet wind tunnel [17] at the Brandenburg University of Technology, using a circular nozzle with an exit diameter of 0.2 m. A photograph of the setup is shown in Figure 1(a), a corresponding schematic in Figure 1(b).

The inflow turbulence required for the generation of leading edge noise was generated using turbulence grids mounted to the wind tunnel nozzle. To generate different turbulent inflow conditions, two perforated plates with square holes (PPS) of different geometry were used. Their parameters are given in Table 1. The grids are the same ones also used in [18]. The different porosities of the two grids, defined as the ratio of the open surface to the total surface, lead to different pressure losses over the grids. In turn, this results in different maximum flow speeds due to the fact that there is an upper limit for the total pressure that can be provided by the fan of the aeroacoustic wind tunnel.

It is known that grid-generated turbulence decays rapidly and is quasi isotropic and homogeneous at a distance of approximately 10 mesh widths downstream of the grid [19]. In the present case, this would correspond to a distance of at least 0.14 m. In the end, a distance of 0.2 m between the turbulence grid and the leading edge of the airfoils was used. In order to determine the parameters of the turbulence at this distance, hot-wire measurements were performed using a Dantec P11 single wire probe and a multi-channel Constant Temperature Anemometry (CTA) measurement system. The probe was positioned by a 3D traverse system made by Isel. To identify any potential inhomogeneity of the turbulence, measurements

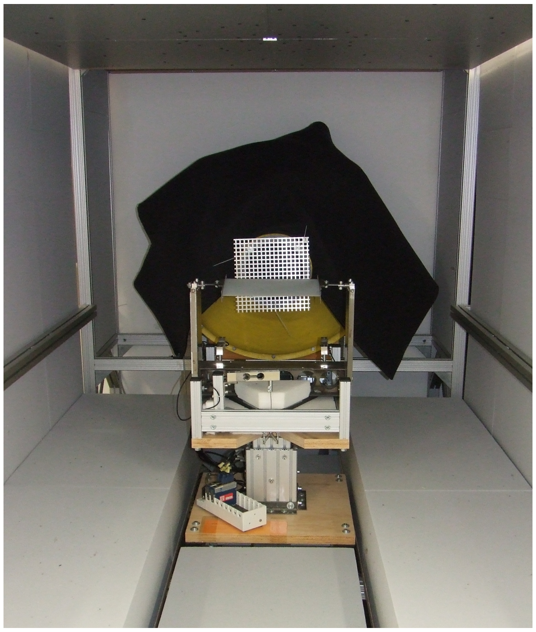

(a) Photograph (taken from downstream direction)

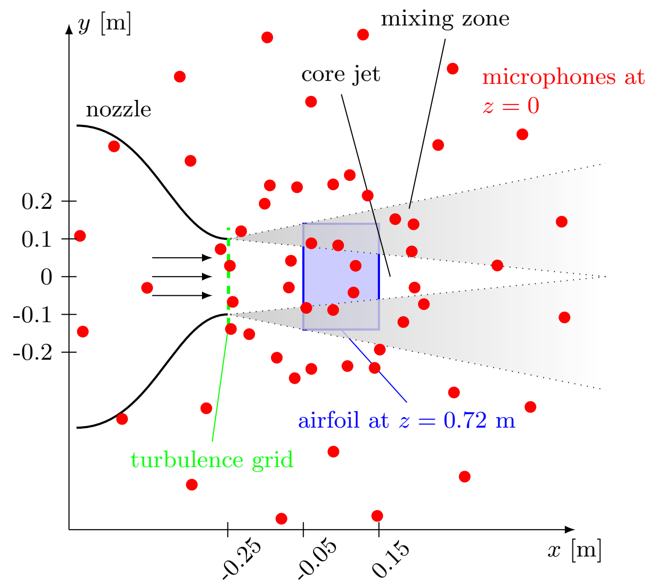

(b) Schematic (top view)

Figure 1. Measurement setup inside the aeroacoustic wind tunnel facility

were conducted at 30 positions randomly distributed on a plane normal to the flow. The data were recorded with a sampling frequency of 25.6 kHz over a measurement duration of 12 s. To avoid the possible influence of vibrations of the traverse system after each step, the first 2 s from each time series were omitted, leaving 256.000 samples to be analyzed. As done in [20], the turbulence length scale Λ_x was determined by fitting the one-sided power spectrum of the velocity fluctuations u to

$$G_{uu}(f) = \frac{4\tilde{u}^2\Lambda_x}{U\left(1+\left(\frac{2\pi f\Lambda_x}{U}\right)^2\right)}, \tag{1}$$

which is a formulation for isotropic and homogeneous turbulence given in [21]. The resulting turbulence intensities and turbulence length scales for both turbulence grids are given in Figures 2(a) and 2(b), respectively.

The first grid, PPS 12/2, produces turbulence with an increasing intensity between 2.6 % at low flow speeds up to 6.2 % at the highest flow speed of 73.3 m/s at this distance. The integral length scale takes values between 4.9 mm and 5.6 mm. The turbulence intensity produced by the second grid, PPS 14/4, does not vary as much with the flow speed. It takes values between 4.7 % and 5.1 %, while the integral length scale is between 5.3 mm and 6.0 mm. For both grids, the standard deviation of turbulence intensity and integral length scale are very small only, confirming that the turbulence at this distance from the grid is nearly homogeneous.

For each turbulence grid, measurements were performed at ten flow speeds (see Figure 2). In addition to the experiments with the two grids from Table 1, measurements were also performed without a turbulence grid. In this case, the turbulence intensity 0.2 m downstream from the nozzle exit is well below 1 %.

The test section is surrounded by a chamber that has absorbing walls on three sides with a microphone array for a ceiling (see Figure 1(a)). The absorbing side walls lead to a quasi-anechoic environment inside the tunnel for frequencies above approximately 125 Hz.

II.B. Leading Edge Hook Structures

To examine the possible reduction of turbulence interaction noise through leading-edge hook structures, six different types of hooks were mounted to the leading edge of a NASA/Langley LS(1)-0413 airfoil. This airfoil, which is a 12.9% thick low speed airfoil used in CART-2 and CART-3 wind turbines, has a chord

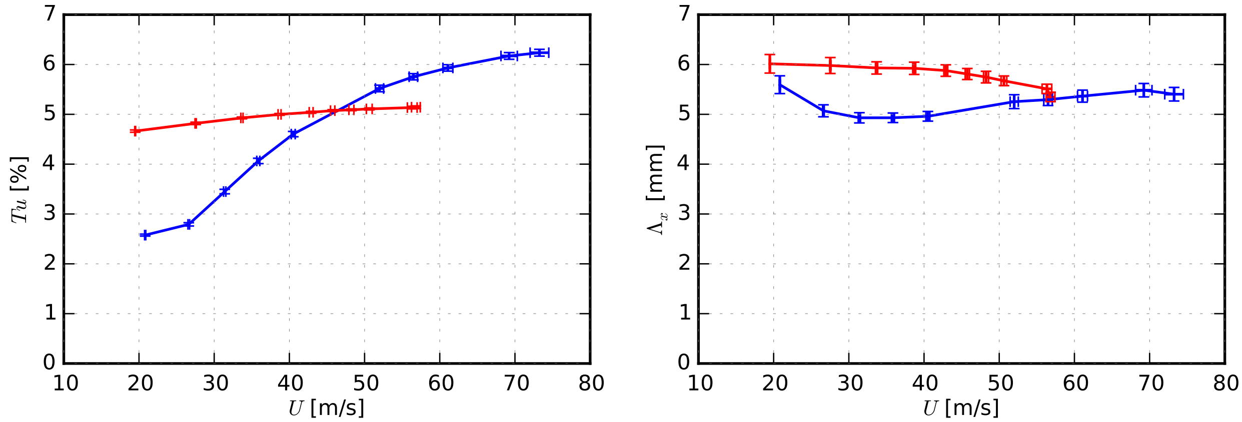

(a) Turbulence intensity (b) Turbulence length scale

Figure 2. Properties of the turbulent inflow generated by the two perforated plates given in Table 1, measured at 30 points in a plane normal to the flow, at the position of the leading edge (given is the mean value as well as the standard deviation), PPS 12/2, PPS 14/4

Table 2. Overview of hook structures used in the experiments

No	hook length [mm]	distance between hooks [mm]	shape
1	20	7.6	straight
2	12	7.6	straight
3	20 / 12 mixed	3.8	straight
4	20	7.6	curved
5	12	7.6	curved
6	20 / 12 mixed	3.8	curved

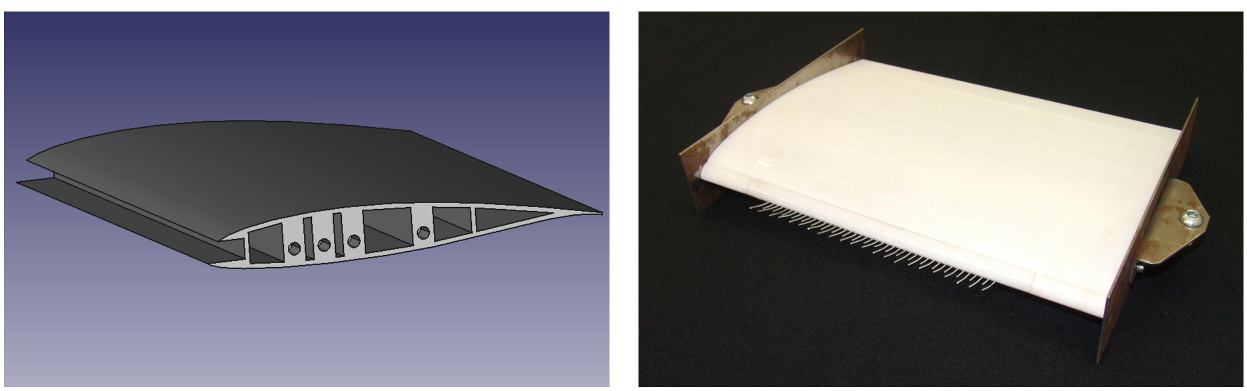

(a) CAD file of the main body (without leading edge inserted) (b) Photograph (with curved hooks of 20 mm and 12 mm length)

Figure 3. Airfoil used for the present investigation

length c_l of 0.2 m and a span width b of 0.28 m. The airfoil was made using Selective Laser Sintering (SLS). It consisted of a main body, shown in Figure 3(a), in which different leading edges can be inserted. Several methods were tried to build the desired leading edge hooks. In the end, the hooks were made from steel pins with a diameter of 0.7 mm, which were stuck inside a leading edge insert that contained regular holes of $\leq$ 0.8 mm diameter. An overview of the hook structures examined in the present study is given in Table 2. Thereby, the pins were not distributed along the complete span of the airfoil, but only over the center part that had a spanwise width of 0.2 m (which corresponds to the exit diameter of the nozzle). Figure 3(b) shows a photograph of the airfoil with curved hooks of 20 mm and 12 mm length.

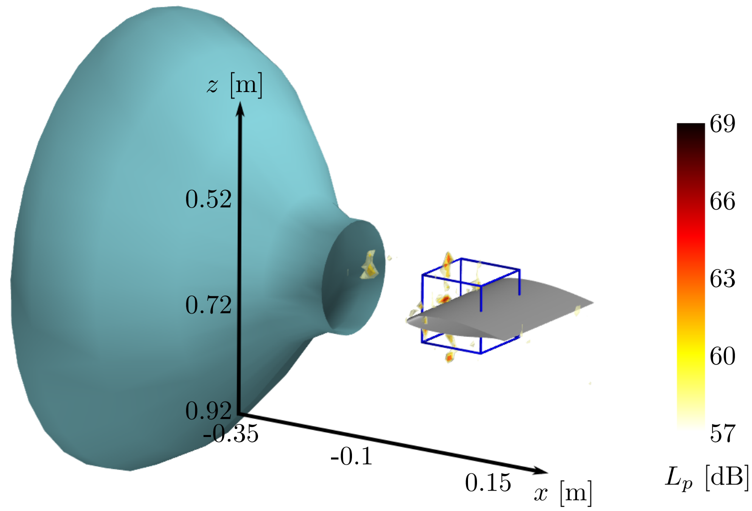

Figure 4. Sample sound map of the noise from the reference airfoil at U_0 = 73.3 m/s, angle of attack 6°, 2 kHz octave band, PPS 12/2 turbulence grid (not shown), including the three-dimensional integration sector (blue cuboid)

Another LS(1)-0413 airfoil, without leading edge modifications, served as a reference, while additional reference measurements were also conducted using a NACA 0012 airfoil of the same chord length and span width. No tripping device was used for the experiments with turbulence grids. For the measurements without grid, both reference airfoils had *anti-slip tape* applied, which has a coarse surface, with a height of approximately 0.8 mm and a width of 5 mm.

II.C. Microphone Array and Data Processing

The acoustic measurements were conducted using a planar 56-channel microphone array, which was positioned 0.72 m above the airfoil and hence out of flow (see Figure 1). For each channel, 40 s of data were recorded with a sampling frequency of 51.2 kHz, using a National Instruments 24 bit multichannel measurement system, and stored. In post-processing the recorded data were first Fourier-transformed into the frequency domain. This was done block-wise with blocks of 4,096 samples length, using a Hanning window and an overlap of 50 %. This lead to 1,000 blocks, for which the results were then averaged to obtain the cross spectral matrix. Secondly, the cross spectral matrizes were further processed using the CLEAN-SC algorithm by Sijtsma [22], which was applied to a fully three-dimensional source region. Thereby, the chosen steering vector was that corresponding to Formulation IV in [23]. The outcomes from this beamforming are three-dimensional maps of acoustic source positions (3D sound maps). A sample sound map is shown in Figure 4.

In order to obtain sound pressure level spectra for the noise generated at the leading edge of the airfoil, all noise sources in the sound map that are positioned within a certain three-dimensional volume were integrated. In the present case, the chosen integration volume has an extent of 0.12 m in all three directions in space and contained only the center part of the leading edge. Unwanted background noise sources, such as the turbulence grid, the airfoil trailing edge or the side regions where the wind tunnel shear layer interacts with the airfoil, where excluded from the integration. The chosen integration volume is visible in Figure 4. Finally, the integrated sound pressures were converted to third octave band sound pressure levels.

II.D. Aerodynamic Measurements

Simultaneously with the acoustic measurements, the aerodynamic performance of the airfoils was captured using a six component balance (visible in Figure 1(a)). The airfoil was attached to the balance at its tips, both of which were outside of the flow. The data from the six load cells were recorded with a sampling frequency of 1 kHz and a measurement duration of 10 s using two National Instruments 24 bit full bridge analog input modules. From these data, the lift and drag forces were calculated (see [24] for details). Due to the fact that the present aerodynamic measurements were performed in an open jet setup, which consists of a cone-shaped core jet with expanding shear layers, the results cannot be directly compared to values obtained

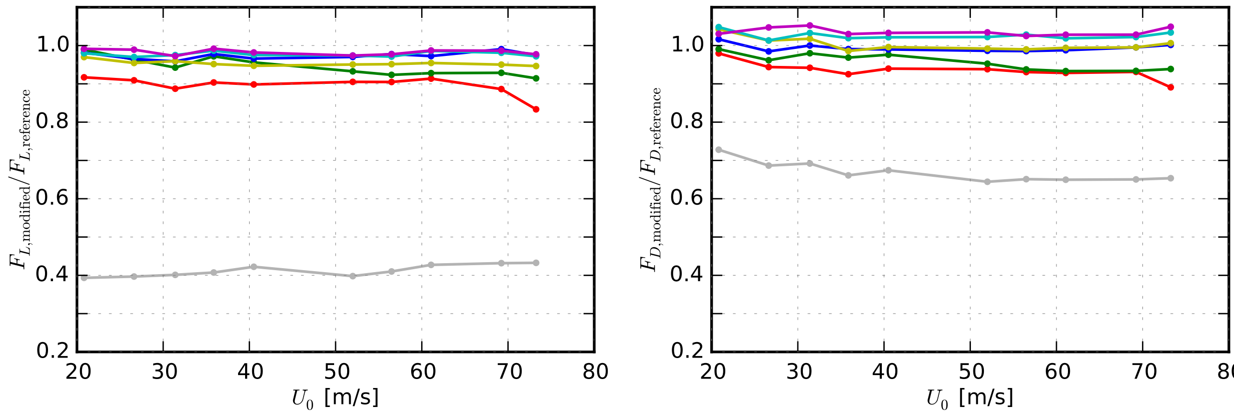

(a) Normalized lift force

(b) Normalized drag force

Figure 5. Aerodynamic forces of the airfoils with different leading edge hook structures, normalized with the corresponding values of the reference LS(1)0413 airfoil, 6° angle of attack (▬ reference NACA 0012, ▬ 20 mm straight, ▬ 12 mm straight, ▬ 20 mm/12 mm straight, ▬ 20 mm curved, ▬ 12 mm curved, ▬ 20 mm/12 mm curved)

in a closed test section. Thus, the measured forces only serve as a means to compare the aerodynamic performance of the modified airfoils with that obtained for the reference airfoil in the same setup.

III. Results and Discussion

Measurements were performed at three geometric angles of attack of 0°, 6° and 12° for both turbulence grids from Table 1 and for the case without a grid. However, in the present paper only acoustic results obtained with the two grids at an angle of attack of 6° will be shown. For each combination of airfoil and turbulence grid, measurements were made at ten flow speeds. As mentioned before, these flow speeds were different for each grid due to the differences in pressure loss.

III.A. Aerodynamic Performance

In this section, the aerodynamic performance of airfoils with different leading edge hook structures will be compared. To this end, Figure 5 shows the measured lift and drag forces of the modified airfoils, normalized with the values of the reference LS(1)0413 airfoil. Thereby, the given results are from measurements with the first turbulence grid from Table 1 (PPS 12/2).

In general, the modifications appear to have only a small influence on the resulting aerodynamics over the complete range of flow speeds. The lift force, shown in Figure 5(a), is highest for the modified airfoils with straight and curved hooks of mixed length (12 mm and 20 mm). The LS(1)0413 airfoil that generates the lowest lift is the one with straight hooks of 20 mm length. At the minimum, it generates about 83 % of the value from the reference airfoil. Also included in Figure 5(a) is the normalized lift force of the NACA 0012 airfoil used as an additional reference, which is considerably lower than that of the LS(1)0413 airfoils regardless of their modification. This is due to the fact that the NACA 0012 is a symmetric airfoil, whereas the LS(1)0413 has a significant camber and thus generates a higher lift.

The measured drag forces are shown in Figure 5(b). The highest drag forces are generated by the airfoil with curved hooks of mixed length and by the airfoil with curved hooks of 12 mm length, with values that exceed those of the reference airfoil. The lowest drag for the modified airfoils was measured for the airfoil with straight 20 mm long hooks, which gives drag forces that are between 89 % and 98 % of the values obtained for the reference airfoil. This means that some of the hook structures lead to an increase in drag, while others actually reduce drag. The drag forces measured for the NACA 0012 airfoil are considerably lower than those of the reference airfoil.

One modified airfoil that gives a high lift force while at the same time does not show an increase in drag is the airfoil with straight hooks of mixed length, although, overall, the aerodynamic performance of all modified LS(1)0413 airfoils is not significantly lower than that of the reference airfoil.

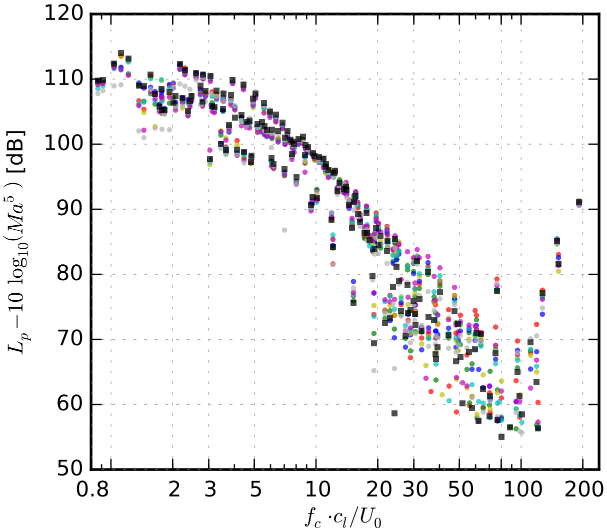

(a) turbulence grid PPS 12/2

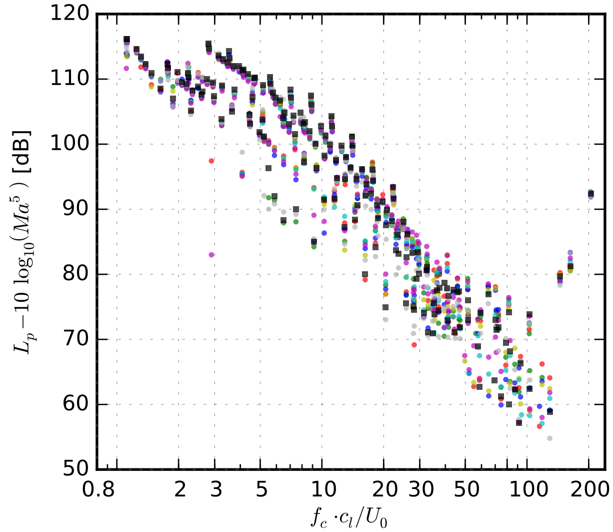

(b) turbulence grid PPS 14/4

Figure 6. Sound pressure levels measured for the different airfoils at 6° angle of attack, scaled with Ma^5 (■ reference LS(1)0413, ● reference NACA 0012, ● 20 mm straight, ● 12 mm straight, ● 20 mm/12 mm straight, ● 20 mm curved, ● 12 mm curved, ● 20 mm/12 mm curved)

III.B. Sound Pressure Levels

The measured third octave band sound pressure levels are shown in Figure 6 for both turbulence grids. They are plotted as a function of the chord-based Strouhal number and scaled using the fifth power of the Mach number. This scaling approach is based on the theoretical work by Ffowcs Williams and Hall [25] and was found to yield good results for the present data.

Overall, the spectra show a maximum at low Strouhal numbers between approximately 0.8 and 3. Then, with increasing Strouhal numbers, the sound pressure levels decrease with about 30 dB per decade. At Strouhal numbers above 120, a strong increase in the spectra can be seen. This increase, which corresponds to third octave band center frequencies above 12.5 kHz, does not seem to be related to any physical noise sources inside the leading edge integration volume. Indeed, sound maps of these frequency bands reveal that the main noise source at such high frequencies is the turbulence grid, while all sources at the airfoil are more than 30 dB below. Hence it is very likely that these sudden high levels are spurious background noise sources, and therefore the analysis of the present data will be limited to third octave bands with center frequencies below 16 kHz.

In a next step, an additional scaling was tested on the data. According to different experimental studies, such as the work by Hutcheson et al. [26], the noise generated at the leading edge of an airfoil subject to a turbulent flow is proportional to the square of the intensity and to the streamwise integral length scale of the turbulence. Correspondingly, Figure 7 shows the scaled third octave band sound pressure levels

$$L_{p,\text{scaled}} = L_p - 10 \cdot \log_{10}\left(\hat{\Lambda}_x \cdot Tu^2 \cdot U^5\right) \text{ dB}. \tag{2}$$

Since dimensionless quantities are required, in Equation (2) the ratio of the streamwise integral length scale to the maximum thickness of the LS(1)-0413 airfoil,

$$\hat{\Lambda}_x = \frac{\Lambda_x}{0.129 \cdot c_l}, \tag{3}$$

is used rather than the integral length scale Λ_x.

When comparing the spectra from Figure 7 with those shown in Figure 6, it becomes apparent that the scaling according to Equation (2) does not deliver substantially better results. In fact, the scatter of the data seems to be even larger. This is especially true for the PPS 12/2 turbulence grid (Figures 6(a) and 7(a)) in a medium Strouhal number range from 3 to 9 and at high Strouhal numbers above 20. The reason

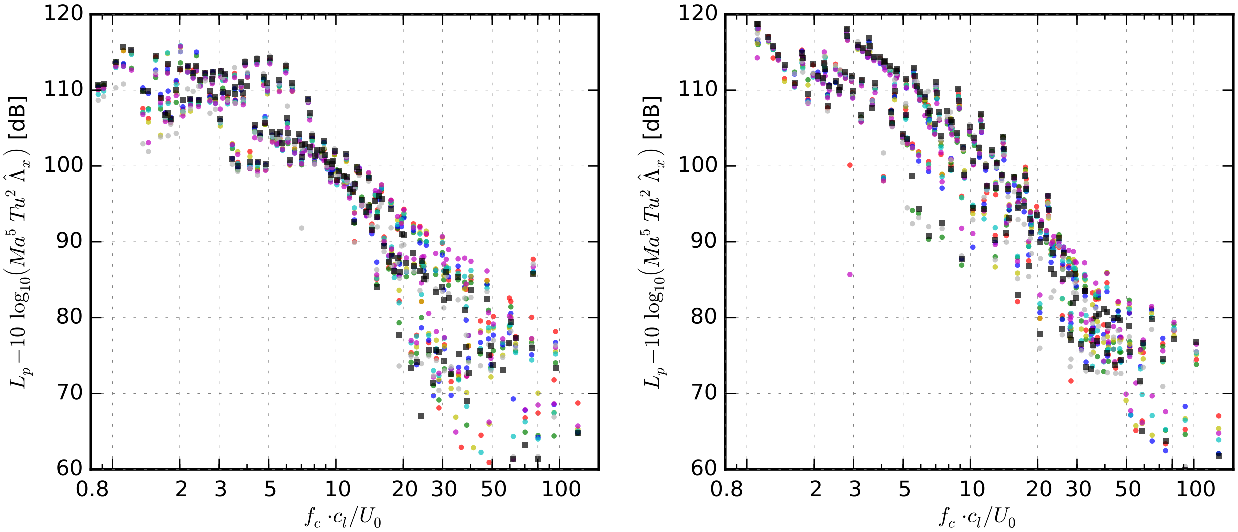

(a) turbulence grid PPS 12/2 (b) turbulence grid PPS 14/4

Figure 7. Sound pressure levels measured for the different airfoils at 6° angle of attack, scaled with $Ma^5 Tu^2 \Lambda_x$ (■ reference LS(1)0413, ● reference NACA 0012, ● 20 mm straight, ● 12 mm straight, ● 20 mm/12 mm straight, ● 20 mm curved, ● 12 mm curved, ● 20 mm/12 mm curved)

for these deviations is most likely the increase of the turbulence intensity with increasing flow speed, shown in Figure 2(a), for the PPS 12/2 grid.

However, regarding the influence of the leading edge hooks structures on the noise generation it can be concluded from Figures 6 and 7 that the effect of the modifications seems to be quite small. Additionally, the scatter of the data makes it hard to determine any clear trend. It is reasonable to assume that the leading edge noise sound pressure levels generated by the airfoils in fact are explicitly dependent on the Strouhal number, and thus it is desirable to represent this relation with a smooth curve instead of a scatter plot. To achieve this, different mathematical algorithms are available which help to enhance the visibility of basic trends or models by removing the scatter of measured data (see for example [27]). One of these routines is the LOWESS algorithm (*locally weighted scatterplot smoothing*) [28], a non-parametric regression method that utilizes low-degree polynomial fits to subsets of the data. Figure 8 shows the resulting Loess curves obtained by applying the algorithm to the scattered data from Figure 6.

Three basic conclusions can now be drawn from these smoothed spectra. Firstly, for a large range of medium Strouhal numbers (approximately between 2 and 20), the modified airfoils generate essentially the same noise as the unmodified reference airfoil. Secondly, at low Strouhal numbers (approximately below 2), the hook structures lead to a noise reduction compared to the reference LS(1)-0413 airfoil. This noise reduction, however, is quite moderate. For the PPS 12/2 turbulence grid, it takes values of up to 2 dB only, while for the PPS 14/4 turbulence grid the reduction is even smaller. It appears that the airfoil with the curved hooks of 12 mm and 20 mm length gives the best noise reduction. Thirdly, at high Strouhal numbers (above 20), the hook structures lead to an increase in noise. This increase is approximately the same order of magnitude as the noise reduction observed at low Strouhal numbers.

It is also visible from Figure 8 that the noise generated by the NACA 0012 airfoil is lower than that generated by the LS(1)-0413 airfoils. This is simply due to the fact that the leading edge of the NACA airfoil is considerably thicker, which is known to be beneficial regarding edge noise generation (see for example [26, 29, 30]).

In order to be able to distinguish the effect of the different modifications more clearly, the sound pressure level differences between the noise generated by the reference LS(1)-0413 airfoil and the noise generated by the modified airfoils,

$$\Delta L_p = L_{p,\mathrm{reference}} - L_{p,\mathrm{modified}}, \tag{4}$$

will be analyzed. The results are shown in Figures 9 and 10 as a function of frequency and chord based Reynolds number. Thereby, the third octave band sound pressure level data were interpolated using a two-dimensional Clough-Tocher scheme [31] in order to obtain a better resolution.

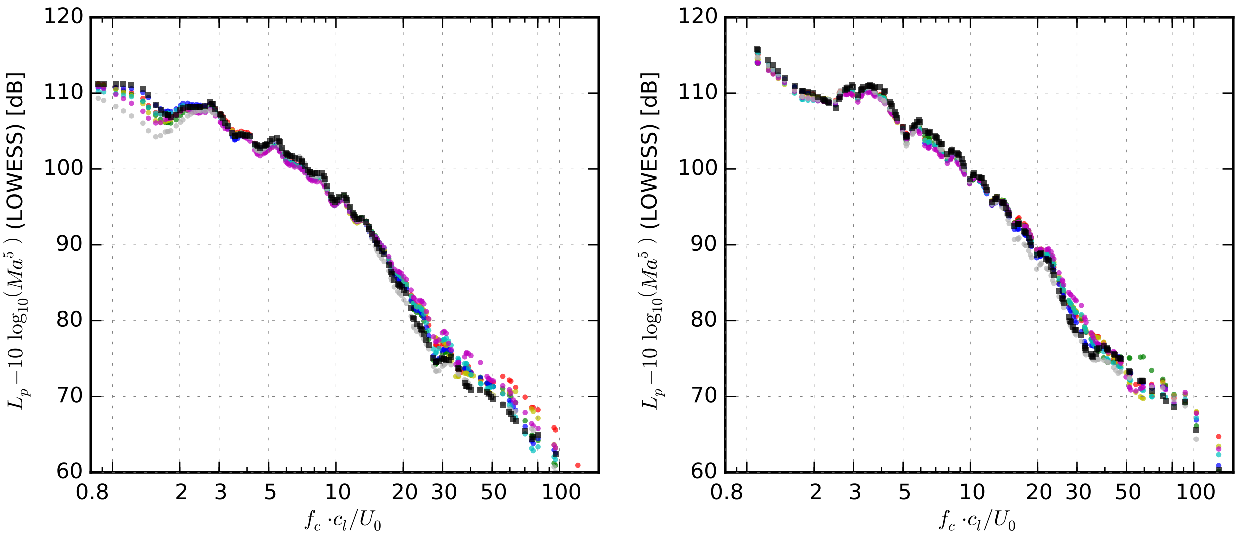

(a) turbulence grid PPS 12/2

(b) turbulence grid PPS 14/4

Figure 8. Sound pressure levels measured for the different airfoils at 6° angle of attack, scaled with Ma^5 and smoothed using a LOWESS algorithm (■ reference LS(1)0413, ● reference NACA 0012, ● 20 mm straight, ● 12 mm straight, ● 20 mm/12 mm straight, ● 20 mm curved, ● 12 mm curved, ● 20 mm/12 mm curved)

From these figures, regions can now be observed in more detail where the modifications lead to a reduction of leading edge noise as opposed to regions where an increase in noise was measured. For the PPS 12/2 turbulence grid (Figure 9) noise reductions appear mainly at low frequencies. The corresponding frequency range increases toward medium frequencies with increasing Reynolds number. At medium frequencies (starting at approximately 1.25 kHz at the lowest Reynolds number), increased noise is observed. However, when increasing the Reynolds number, the lower frequency limit of the region in which this increase is found gradually increases. Finally, at the highest Reynolds numbers, no noticeable increase of noise occurs at medium frequencies. At frequencies above approximately 6.3 kHz, it is difficult to make conclusion about the emitted noise, since several, smaller regions of noise reduction and regions of noise increase are visible. It can be observed qualitatively, though, that the airfoil with the curved hooks of 12 mm and 20 mm length seems to give the best performance regarding a low noise emission.

In case of the PPS 14/4 turbulence grid (Figure 10), similar conclusions can be drawn as for the PPS 12/2 grid. However, an additional region of strong noise increase becomes visible in a frequency range between approximately 1.0 kHz and 1.6 kHz. It is present at low and medium Reynolds numbers up to approximately 640,000. Only the results for the airfoils with the straight hooks of 12 mm length do not feature this region, making this the airfoil that performs best in this case. The reason for this is not yet known.

The fact that the modifications lead to a noise reduction at low frequencies combined with a noise increase at high frequencies, which is evident in Figures 8, 9 and 10, allows for conclusions on the probable working principle of the leading edge hooks. It is reasonable to assume that the hook structures break up the incoming turbulent eddies, effectively reducing their size until they are in the order of magnitude of the spacing between the pins. Since the size of the eddies is related to the frequency range of the emitted leading edge noise (large eddies generate low frequency noise, while small eddies generate high frequency noise, see for example [32]), this break-up leads to the observed frequency shift. Therefore, a main outcome of the present study is that an even smaller spacing between the pins is desirable, which would then shift a longer portion of the low frequency turbulence interaction noise toward higher frequencies.

Another conclusion that can be drawn from the present results is that the increase in noise reduction with increasing Reynolds number does not seem to be strictly limited. This means that for real wind turbine blades, which usually operate at higher Reynolds numbers, the noise reducing effect of the examined hook structures may be more significant.

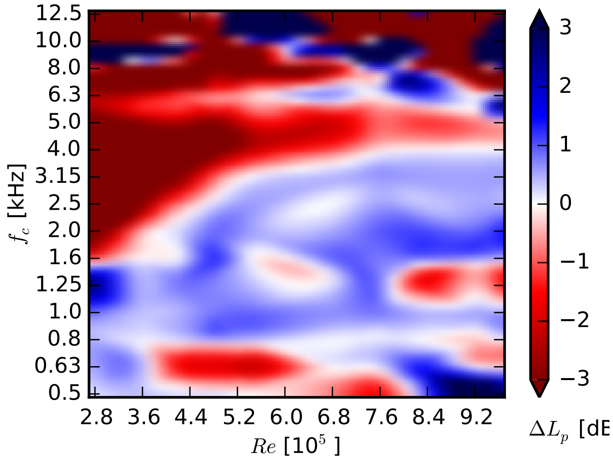

(a) Straight hooks, 20 mm

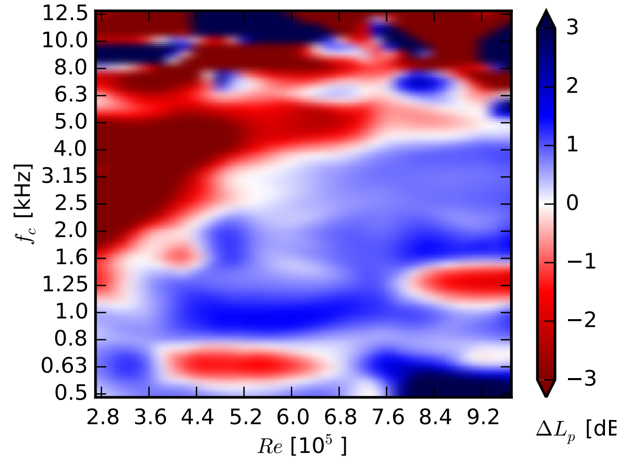

(b) Curved hooks, 20 mm

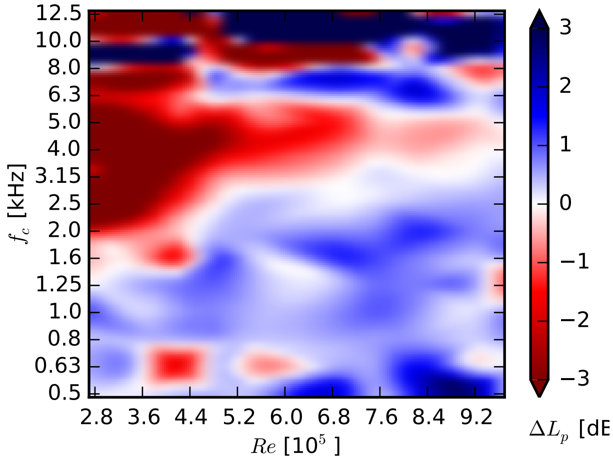

(c) Straight hooks, 12 mm

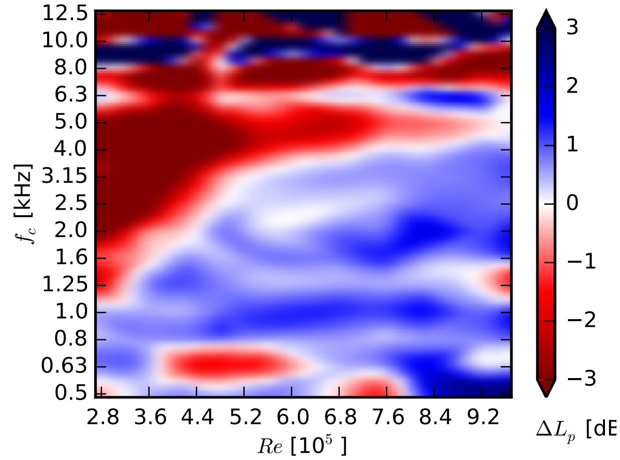

(d) Curved hooks, 12 mm

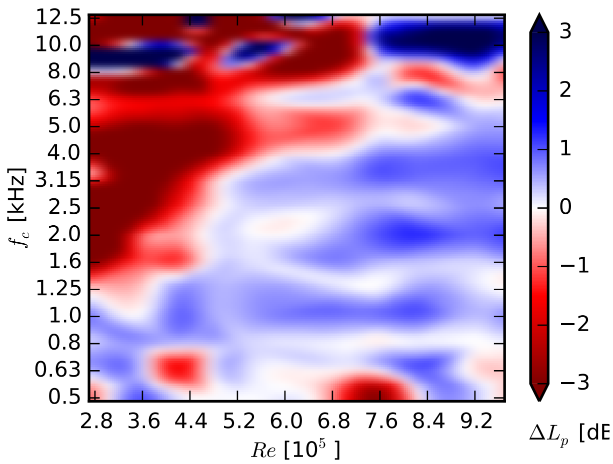

(e) Straight hooks, 20 mm and 12 mm (mixed)

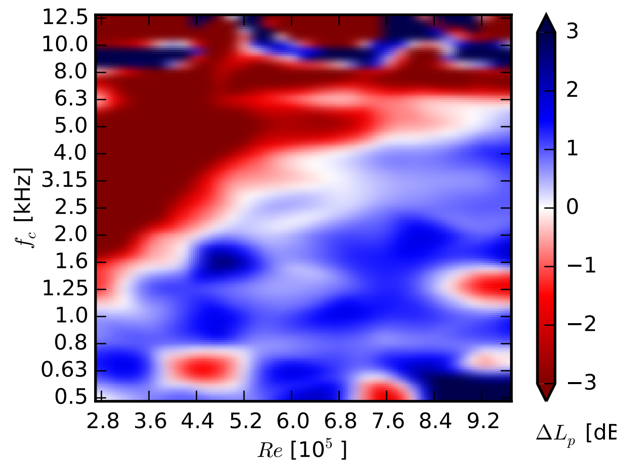

(f) Curved hooks, 20 mm and 12 mm (mixed)

Figure 9. Sound pressure level difference between airfoils with leading edge hook structures and reference airfoil without modifications, angle of attack 6°, PPS 12/2 turbulence grid (positive values denote a noise reduction due to the modifications, negative values a noise increase)

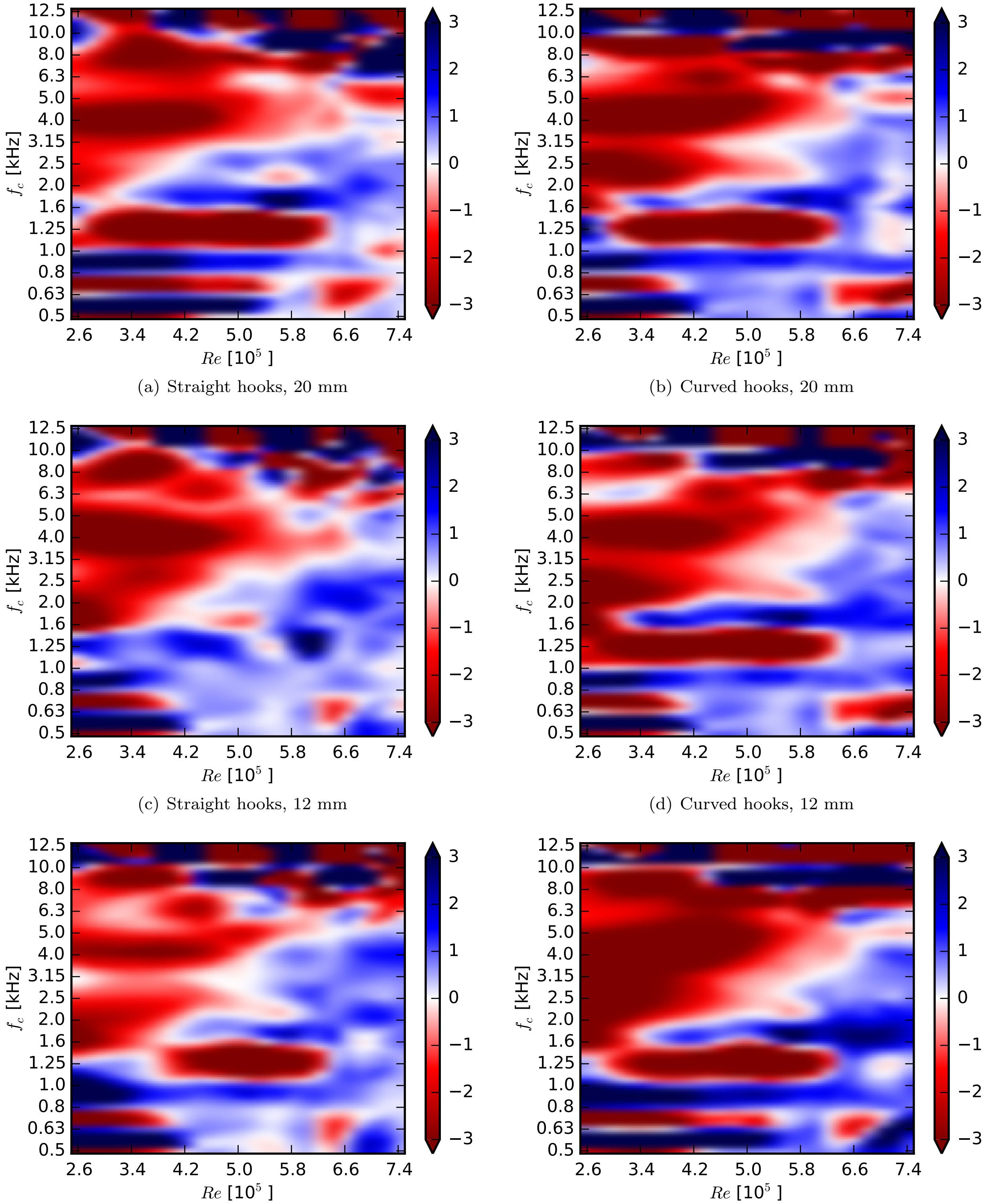

(a) Straight hooks, 20 mm

(b) Curved hooks, 20 mm

(c) Straight hooks, 12 mm

(d) Curved hooks, 12 mm

(e) Straight hooks, 20 mm and 12 mm (mixed)

(f) Curved hooks, 20 mm and 12 mm (mixed)

Figure 10. Sound pressure level difference between airfoils with leading edge hook structures and reference airfoil without modifications, angle of attack 6°, PPS 14/4 turbulence grid (positive values denote a noise reduction due to the modifications, negative values a noise increase)

IV. Summary

An experimental study was performed to explore the effect of hook-like extensions at the leading edge of airfoils on the generation of turbulence interaction noise. The study took place in a small aeroacoustic wind tunnel, where the required turbulent inflow was generated by two different perforated plates. The airfoils of the type LS(1)-0413 had leading edges that were modified with steel pins, thus creating a comb-like structure. The length and distance of the pins, which were either straight or slightly curved in an upward manner, was varied.

The results from the aerodynamic measurements showed that the hook structures do not change the aerodynamic performance significantly. The results from the acoustic measurements showed that, overall, the influence of the hook structures is small. A noise reduction was observed at low frequencies approximately below 1.6 kHz, while at the same time more noise is generated at high frequencies. This leads to the conclusion that the function of the hooks is to break up the incoming turbulent eddies, thereby reducing their size, which leads to a shift in the noise generated at the leading edge from lower to higher frequencies.

In general, the modifications that performed best in terms of noise reduction and aerodynamic performance are hooks with mixed length and a very small spacing between the single pins. Future experiments should be conducted using hook structures that have even smaller spacings, as it is assumed that the size of the turbulent eddies after they pass the hooks would be smaller, thus shifting the noise to even higher frequencies.

Acknowledgements

The participation at the 22nd AIAA/CEAS Aeroacoustics Conference 2016 was financially supported by the German Academic Exchange Service *DAAD*, which is gratefully acknowledged.

References

[1]Wasala, S. H., Storey, R. C., Norris, S. E., Cater, J. E., Aeroacoustic noise prediction for wind turbines using Large Eddy Simulation. Journal of Wind Engineering and Industrial Aerodynamics, 17-29 (2015)

[2]Hersh, A. S., Sodermant, P. T., Hayden, R. E., Investigation of acoustic effects of leading-edge serrations on airfoils. Journal of Aircraft, 11(4), 197 - 202 (1974)

[3]Roger, M., Schram, C., De Santana, L., Reduction of airfoil turbulence-impingement noise by means of leading-edge serrations and/or porous materials. 19th AIAA/CEAS Aeroacoustics Conference (34th AIAA Aeroacoustics Conference). AIAA-Paper 2013-2108 (2013)

[4]Chaitanya, P., Narayanan, S., Joseph, P., Vanderwel, C., Turner, J., Kim, J. W., Ganapathisubramani, B., Broadband noise reduction through leading edge serrations on realistic aerofoils. 21st AIAA/CEAS Aeroacoustics Conference, AIAA-Paper 2015-2202 (2015)

[5]Chen, W., Qiao, W., Wang, L., Tong, F., Wang, X., Rod-airfoil interaction noise reduction using leading edge serrations. 21st AIAA/CEAS Aeroacoustics Conference, AIAA-Paper 2015-3264 (2015)

[6]Chong, T. P., Vathylakis, A., McEwen, A., Kemsley, F., Muhammad, C., Siddiqi, S., Aeroacoustic and aerodynamic performances of an aerofoil subjected to sinusoidal leading edges. 21st AIAA/CEAS Aeroacoustics Conference, AIAA-Paper 2015-2200 (2015)

[7]Narayanan, S., Chaitanya, P., Haeri, S., Joseph, P., Kim, J. W., Polacsek, C., Airfoil noise reductions through leading edge serrations. Physics of Fluids, 27(2) (2015)

[8]Geyer, T. F., Sarradj, E., Giesler, J., Hobracht, M., Experimental assessment of the noise generated at the leading edge of porous airfoils using microphone array techniques. 17th AIAA/CEAS Aeroacoustics Conference, AIAA-Paper 2011-2713 (2011)

[9]Kim, J. W., Haeri, S., Joseph, P. F., On the mechanisms of noise reduction in aerofoil-turbulence interaction by using wavy leading edges. 21st AIAA/CEAS Aeroacoustics Conference, AIAA-Paper 2015-3269 (2015)

[10]Mathews, J., Peake, N., Noise generation by turbulence interacting with an aerofoil with a serrated leading edge. 21st AIAA/CEAS Aeroacoustics Conference, AIAA-Paper 2015-2204 (2015)

[11]Lee, S., Reduction of blade-vortex interaction noise through porous leading edge. AIAA Journal, 32, 480 - 488 (1994)

[12]Wasala, S. H., Norris, S. E., Cater, J. E., Wind turbine noise reduction by blade geometry modification. 22nd International Congress on Sound and Vibration, Florence, Italy (2015)

[13]Graham, R. R., The silent flight of owls. Journal of the Royal Aeronautical Society, 286, 837 - 843 (1934)

[14]Hertel, H., Struktur, Form, Bewegung. Otto Krauskopf-Verlag Mainz (1963) [translated version: Milton S. Katz (ed.), Structure, form, movement. Reinhold, New York (1966)]

[15]Lilley, G. M., A study of the silent flight of the owl. 4th AIAA/CEAS Aeroacoustics Conference, Toulouse, France, AIAA-Paper 1998-2340 (1998)

[16]Geyer, T. F., Claus, V. T., Sarradj, E., Markus, P. M., Silent Owl Flight: The Effect of the Leading Edge Comb on the Gliding Flight Noise. 22nd AIAA/CEAS Aeroacoustics Conference, AIAA-Paper 2016-3017 (2016)

[17]Sarradj, E., Fritzsche, C., Geyer, T. F., Giesler, J., Acoustic and aerodynamic design and characterization of a small-scale aeroacoustic wind tunnel, Appl Acoust, 70, 1073 - 1080 (2009)

[18]Geyer, T. F., Sarradj, E., Giesler, J., Application of a beamforming technique to the measurement of airfoil leading edge noise. Adv Acoust Vib, Vol. 2012 (2012)

[19]Roach, P. W., The generation of nearly isotropic turbulence by means of grids. J Heat Fluid Flow 8 (2): 82 - 92 (1987)

[20]Sarradj, E., Geyer, T. F., Symbolic regression modeling of noise generation at porous airfoils. Journal of Sound and Vibration, Volume 333, Issue 14, 3189-3202 (2014)

[21]Hinze, J. O., Turbulence, 2nd ed. McGraw-Hill, New York (1975)

[22]Sijtsma, P. CLEAN based on spatial source coherence. International Journal of Aeroacoustics, 6(4), 357-374 (2007)

[23]Sarradj, E.,Three-dimensional acoustic source mapping with different beamforming steering vector formulations. Adv Acoust Vib, Vol. 2012 (2012)

[24]Geyer, T. F., Trailing edge noise generation of porous airfoils. PhD-Thesis, Brandenburg University of Technology Cottbus (2011)

[25]Ffowcs Williams, J. E., Hall, L. H., Aerodynamic sound generation by turbulent flow in the vicinity of a scattering half plane, Journal of Fluid Mechanics, 40, 4, 657 - 670 (1970)

[26]Hutcheson, F. V., Brooks, T. F., Stead, D. J., Measurement of the noise resulting from the interaction of turbulence with a lifting surface. International Journal of Aeroacoustics, 11(5), 675-700 (2012)

[27]Martinez, W. L., Martinez, A., Solka, J., Exploratory data analysis with MATLAB. CRC Press (2010)

[28]Cleveland, W. S., Robust locally weighted regression and smoothing scatterplots. Journal of the American Statistical Association, 74, 829-836 (1979)

[29]Gershfeld, J., Leading edge noise from thick foils in turbulent flows. Journal of the Acoustical Society of America, 116(3), 1416 - 1426 (2004)

[30]Chaitanya, P., Gill, J., Narayanan, S., Joseph, P., Vanderwel, C., Zhang, X., Ganapathisubramani, B., Aerofoil geometry effects on turbulence interaction noise. 21st AIAA/CEAS Aeroacoustics Conference, AIAA-Paper 2015-22830 (2015)

[31]Alfeld, P., A trivariate Clough-Tocher scheme for tetrahedral data. Computer Aided Geometric Design, 1, 169 (1984); G. Farin, Triangular Bernstein-Bezier patches. Computer Aided Geometric Design, 3, 83 (1986)

[32]Wagner, S., Bareiss, R., Guidati, G., Wind turbine noise. Springer Science & Business Media, (2012)